

J1420–0545: The radio galaxy larger than 3C236

J. Machalski¹

machalsk@oa.uj.edu.pl

D. Koziel-Wierzbowska¹

eddie@oa.uj.edu.pl

M. Jamrozy¹

jamrozy@oa.uj.edu.pl

D.J. Saikia²

djs@ncra.tifr.res.in

¹ *Astronomical Observatory, Jagellonian University, ul. Orła 171, PL-30244 Krakow, Poland*

² *National Centre for Radio Astrophysics, Tata Institute of Fundamental Research (TIFR), Pune University Campus, Post Bag 3, Pune 411 007, India*

ABSTRACT

We report the discovery of the largest giant radio galaxy, J1420-0545: a FR type II radio source with an angular size of 17.4' identified with an optical galaxy at $z=0.3067$. Thus, the projected linear size of the radio structure is 4.69 Mpc (if we assume that $H_0=71 \text{ km s}^{-1}\text{Mpc}^{-1}$, $\Omega_m=0.27$, and $\Omega_\Lambda=0.73$). This makes it larger than 3C236, which is the largest double radio source known to date. New radio observations with the 100 m Effelsberg telescope and the Giant Metrewave Radio Telescope, as well as optical identification with a host galaxy and its optical spectroscopy with the William Herschel Telescope are reported. The spectrum of J1420–0545 is typical of elliptical galaxies in which continuum emission with the characteristic 4000 Å discontinuity and the H and K absorption lines are dominated by evolved stars. The dynamical age of the source, its jets' power, the energy density, and the equipartition magnetic field are calculated and compared with the corresponding parameters of other giant and normal-sized radio galaxies from a comparison sample. The source is characterized by the exceptionally low density of the surrounding IGM and an unexpectedly high expansion speed of the source along the jet axis. All of these may suggest a large inhomogeneity of the IGM.

Subject headings: galaxies: active – galaxies: distances and redshifts – galaxies: individual (J1420–0545)

1. Introduction

The existence of bright hot spots at the edges of most of FR type II radio sources indicates that the jets ejected from a "central engine" in the AGN encounter resistance to their propagation. These supersonically advancing hotspots are likely to be confined by the ram pressure of the external environment, which on the largest scales is the intergalactic medium (IGM). The shocked jet material and shocked IGM form a cocoon surrounding the pair of jets. In a number of FR type II radio sources, such a cocoon is observed as a low-brightness bridge between the radio lobes (Leahy & Williams 1984). While the lengthening of the cocoon is governed by the balance between the jet's thrust and the ram pressure of the IGM, the width of the cocoon is determined by its mean internal pressure, which is on the order of the kinetic energy delivered by the jets divided by the cocoon's volume. As both of these factors are functions of time, it is possible that the lateral expansion of the cocoon could be faster than the rate at which the jets delivered energy. Thus, the cocoon's pressure would decrease until it reached an equilibrium with the IGM pressure. However, in a number of papers (e.g. Begelman & Cioffi 1989; Daly 1990; Wellman et al. 1997) there are arguments that the cocoons in many observed radio sources are still overpressured with respect to the IGM. Only the very tenuous material in the bridges of the oldest and largest sources is expected to have attained such an equilibrium state, in which the radiating particles and the magnetic field are balanced, and the pressure of the relativistic plasma equals the pressure of the gaseous environment (cf. Nath 1995). Consequently, a determination of the physical conditions in these diffuse bridges of large-size double radio sources (as they are far away from the ram pressure-confined heads of the source) gives us an independent tool with which to probe the pressure of the IGM.

The above approach was applied by us (Machalski et al. 2007b) to a sample of giant radio galaxy (GRG) candidates located in the southern sky hemisphere with the aim of studying properties of the cosmological evolution of the IGM. The radio galaxy discussed in this paper is a member of that sample. The source J1420–0545 was discerned in the VLA 1.4 GHz surveys FIRST (Becker et al. 1995) and NVSS (Condon et al. 1998) as a 17.4' large FR type II radio structure consisting of two extended lobes with a total flux density of only 87 mJy and a central compact core. The core is unresolved with the $5'' \times 5''$ beam in the FIRST survey and has a flux density of 2.7 mJy. The structure is highly collinear and symmetric; the ratio of separation between the core and the brightest regions in the lobes is 1.08, and the

misalignment angle is 1.3° . The FIRST map reveals also compact hot spots in both lobes, which implies strong shocks and *in situ* reacceleration of relativistic particles, finally inflating the lobes. In order to check whether the observed lobes are or are not possibly connected by a bridge undetected in the NVSS because of the lack of short baselines, we made supplementary single-dish 21 cm observations using the Effelsberg 100 m radiotelescope,¹ as well as 50 cm observations with the Giant Metrewave Radio Telescope (GMRT).² These observations, the final 1.4 GHz map of the investigated radio galaxy obtained from a combination of the NVSS and Effelsberg data, and the 619 MHz GMRT map are presented in § 2. The radio core position coincides perfectly with that of a galaxy with $R \sim 19.65$ mag and $B \sim 21.82$ mag at R.A.(J2000.0) = $14^{\text{h}}20^{\text{m}}23.80^{\text{s}}$ and decl.(J2000.0) = $-05^\circ45'28.8''$, according to the magnitude calibration and astrometric position in the Digitized Sky Survey (DSS) data base. This DSS red magnitude suggests a rather distant galaxy whose photometric redshift estimate would be between 0.46 and 0.42, according to the Hubble diagrams for GRGs published by Schoenmakers et al. (1998) and Lara et al. (2001), respectively. However, the standard deviations in the apparent-magnitude distributions in those diagrams for a given redshift are about 1 mag. Therefore, supposing that the absolute magnitude M_R of galaxies identified with very faint GRGs can be 1σ lower than the mean value, we have estimated a value of $z \approx 0.32$ for J1420–0545 (cf. Machalski et al. 2007b). The independent photometry and optical spectroscopy of the host galaxy that confirm the above estimate are given in § 3, while some physical parameters and the dynamical age of the radio structure are estimated and discussed in § 4.

2. New radio observations

2.1. Effelsberg observations

The observations were carried out with the 100 m telescope on 2006 April 26–27, using the 21 cm single-horn receiver installed at the primary focus of the antenna. The $60' \times 60'$ sky area centred at R.A.(J2000.0)= $14^{\text{h}}20^{\text{m}}24^{\text{s}}$ and decl.(J2000.0)= $-05^\circ45'29''$ was scanned alternately in right ascension and declination. The drive rate was $180'$ per minute and the scan interval was $3'$. For the flux density calibration, the standard source 3C286 was observed. The final Effelsberg map is a combination of the $60' \times 60'$ images, which were large enough to

¹The Effelsberg 100m telescope is operated by the Max-Planck-Institut für Radioastronomie (Bonn, Germany)

²The GMRT is a national facility operated by the National Centre for Radio Astrophysics of the Tata Institute of Fundamental Research (Pune, India)

cover the target source and some emission-free areas used for the zero-level determination. A combination of the Effelsberg and NVSS images was performed using the IMERG task included in the NRAO AIPS package. The resulting 1.4 GHz map of the source J1420–0545, superposed on the optical DSS image, is shown in Figure 1. We still do not detect a bridge at this frequency.

2.2. GMRT observations

The observations of J1420–0545 centered at the radio core position were carried out on 2007 November 11, in the 50 cm band. The observations were made in the standard manner, with observations of the target source interspersed with observations of the phase calibrator J1351–148. The total observing time spent on the source was approximately 6 hr. Again the primary flux density and bandpass calibrator was 3C286. The data were edited, calibrated, and imaged using the standard AIPS routines. Phase self-calibration was done for several rounds to improve the quality of the source’s image. Finally, the image was corrected for the primary beam pattern of the antennas. The data were imaged with different angular resolutions. The tapered 619 MHz map with a resolution of $45'' \times 45''$ (i.e., with resolution identical to that of the NVSS) and an rms noise level of about $0.5 \text{ mJy beam}^{-1}$ is shown in Figure 2. This map also shows no bridge with a surface brightness exceeding the above rms noise level; however, it indicates that the radio core has a very flat spectrum, as its 619 MHz flux density is likely below 1.3 mJy .

3. Optical observations

To check the DSS apparent magnitudes and to derive an absolute magnitude of the host galaxy, an independent photometry was made at Mount Suhora Observatory with the 60 cm telescope. After the initial standard reductions, aperture photometry was performed on the galaxy and calibration stars using the IRAF package APPHOT. The resulting magnitudes in the *UBVRI* photometric system, corrected for the atmospheric extinction only (as the Galactic latitude of this galaxy is 50° , the foreground Galactic extinction is close to zero), are $I=18.44 \pm 0.08 \text{ mag}$, $R=19.65 \pm 0.08 \text{ mag}$, and $V=21.0 \pm 0.2 \text{ mag}$. Thus, our photometry is fully compatible with the DSS magnitudes. The combined data give an optical spectral index of -3.45 and an absolute red magnitude M_R of -22.1 ± 0.1 , if we use the cosmological parameters given in the Abstract.

The optical spectra of the host galaxy were obtained at La Palma on 2007 August

16. The observations conducted in the Service Programme mode were made with the ISIS double beam spectrograph (the red and blue arms) on the 4.2 m William Herschel Telescope (WHT).³ The galaxy was observed in good weather and seeing conditions through a 2'' wide slit. Four spectra (two per arm) were taken with the grating R316R, set up for a central wavelength of 6447Å and a dispersion of 0.92Å pixel⁻¹ at the red arm, and the grating R300B, set up for a central wavelength of 4503Å and a dispersion of 0.86Å pixel⁻¹ at the blue arm. The exposure time for each spectrum was 1800 s. The spectra combined from both arms cover the wavelength range 3400Å–8500Å.

The obtained spectra were reduced using the standard IRAF LONGSLIT package. All the spectra were corrected for bias, flat fields, and cosmic rays, as well as being wavelength- and flux density-calibrated. The wavelength calibration was performed by using exposures to CuAr/CuNe arc lamps, wherea the flux calibration was performed by using exposures of the spectrophotometric standard star SP 1545+035. The standard star was observed directly before and after the target galaxy. The spectra from each arm were averaged separately and were then combined into a common one-dimensional spectrum shown in Figure 3a. The spectrum is typical of elliptical galaxies whose continuum emission with the characteristic 4000 Å discontinuity and *H* and *K* absorption lines is dominated by evolved stars. The spectrum of the S0-type galaxy UGC 04345, as a typical spectrum of an early morphological type galaxy, is shown in Figure 3b for comparison's sake. A Gaussian profile was fitted to the lines and bands recognized in the spectrum, and the wavelengths corresponding to the profile centers are used to calculate the redshift. The emission line and absorption bands detected, as well as the resulting redshifts of these features, are listed in Table 1. If we average the values in column (3) of Table 1, we find that the redshift of J1420–0545 is $z=0.3067\pm 0.0005$.

4. Physical parameters and dynamical age

Given the spectroscopic redshift, we can determine observational parameters that characterize the GRG reported; i.e., the linear size, D , and the volume of the cocoon, V_c , via the axial ratio AR, and radio luminosity, P_ν . Other physical parameters are derived by modeling dynamics of the source with the DYNAGE algorithm (Machalski et al. 2007a). This algorithm is an extension of the analytical model for the evolution of FR type II radio sources, combining the dynamical model of Kaiser & Alexander (1997) with the model for expected radio emission from a source under the influence of energy loss processes published

³The WHT is operated by the Isaac Newton Group in the Spanish Observatorio del Roque de Los Muchachos of the Instituto de Astrofisica de Canarias

by Kaiser et al. (1997, hereafter KDA). The DYNAGE algorithm allows us to determine the values of five of the model parameters, i.e., the jet power, Q_{jet} , central core density, ρ_0 , internal pressure in the cocoon, p_c , dynamical age, t , and initial (injected) spectral index, α_{inj} ; however, there are only four independent parameters, since any combination of three parameters from the set Q_{jet} , ρ_0 , p_c , and t uniquely determines the remaining fourth parameter. The determination of their values is made possible by the fit to the observational parameters of a source: D , AR , P_ν , and the radio spectrum (α), which usually provides P_ν at a number of observing frequencies $\nu = 1, 2, 3, \dots$. The values of other free parameters of the model have to be assumed.

4.1. Linear size, volume, and luminosity

The high symmetry of the radio structure and the weak strength of the core suggests that an inclination angle of the jet axis towards the observer’s line of sight is large, possibly close to 90° . Thus, the linear size of J1420–0545 is $D=4690$ kpc; i.e. it is larger than the measurement of 4380 kpc for 3C236, the largest GRG known (with an angular extent of $2430''$ and a redshift of 0.09883). For the dynamical considerations, the volume of the source is needed. In KDA and DYNAGE a cylindrical geometry of the radio cocoon is assumed; thus, $V_c=\pi D^3/(4AR^2)$. Following Leahy & Williams (1984), we measure the axial ratio AR as the ratio between the angular size of the total structure and the average of the full width (w) of its two lobes. The latter is determined as the largest deconvolved width of the transversal cross section through the lobes measured between 3σ total-intensity contours. We find values of $w \approx 390$ kpc and $AR \approx 12$; however, this latter value is likely an upper limit for the axial ratio, because the cocoon’s width further down towards the core can be larger than the width of the detected lobes. The dependence of age and other physical parameters of J1420–0545 on the value of AR is considered in the next subsection. The 619 MHz and 1400 MHz luminosities are $P_{619} = 3.60 \times 10^{24} \text{ W Hz}^{-1}\text{sr}^{-1}$ and $P_{1400} = 2.06 \times 10^{24} \text{ W Hz}^{-1}\text{sr}^{-1}$, respectively. Because of the limited radio data, the model parameters derived in the next subsection are fitted using the above two luminosity values only.

4.2. Age and other parameters

The model requires the density distribution of the ambient medium (which is invariant with redshift) to be modeled by a power law, $\rho_a(r)=\rho_0(r/a_0)^{-\beta}$, where a_0 is the core radius and the exponent β describes the density profile. With this assumption, the age of a radio structure of linear size D is

$$t \propto D^{\frac{5-\beta}{3}} \left(\frac{\rho_0 a_0^\beta}{Q_{\text{jet}}} \right)^{1/3},$$

the pressure within the cocoon is

$$p_c \propto \left(\rho_0 a_0^\beta \right)^{3/(5-\beta)} Q_{\text{jet}}^{(2-\beta)/(5-\beta)} t^{(-4-\beta)/(5-\beta)},$$

and the energy density and the corresponding equipartition magnetic field strength are

$$u_c [J m^{-3}] = p_c / (\Gamma_c - 1); \quad B_c [nT] = \left(\frac{24}{7} 10^{11} \pi u_c \right)^{1/2},$$

where Γ_c is the adiabatic index of the lobes' (cocoon) material. If we take the same values of the model's free parameters as in Machalski et al. (2007a), in particular $a_0=10$ kpc, $\beta=1.5$, and $\Gamma_c=5/3$, the values of Q_{jet} , ρ_0 , and p_c are determined by the fit to the observed luminosities and volume of the source (cf. KDA). But that fit depends on α_{inj} . In the KDA model this also has to be assumed; however, the DYNAGE algorithm allows us to find its value through a search for the minimum energy density (u_c), which, in turn, is proportional to the minimum kinetic energy delivered to the source (cocoon) by the jets during its actual age; i.e., $2Q_{\text{jet}} t$. The fitted values of Q_{jet} and ρ_0 for $\alpha_{\text{inj}} = 0.48$ and different hypothetical ages of J1420–0545 are shown in the $\log Q_{\text{jet}}-\log \rho_0$ diagram in Figure 4a. The two pairs of curves (solid and dashed) give the fits for two different values of AR; the one determined from the width of the observed lobes (cf. §4.1), and the same, but decreased by a factor of 1.5. This figure shows that both pairs of curves corresponding to two different observing frequencies intersect each other at a similar age of 45–50 Myr. Thus, by enlarging the cocoon's volume by a factor of $(1.5)^2$, we find a significant decrease of the core density ρ_0 compared with that for AR=12, while the values of the age t and Q_{jet} remain comparable.

The dependence of the resulting model solutions of t , Q_{jet} , ρ_0 , and $Q_{\text{jet}}t$ on α_{inj} for AR=12 is shown in Figure 4b. The vertical line and the arrow indicate the value of α_{inj} that corresponds to the minimum value of the product $Q_{\text{jet}}t$. The minimum of this product, which gives the kinetic energy delivered to the cocoon by the jet, corresponds to a minimum of the energy density in the cocoon, u_c , as is expected from the KDA model assumption of energy equipartition between magnetic fields and particles. The parameter values resulting from the fit, as well as their errors, are listed in Table 2 and are compared with the corresponding values derived for 3C236 (J. Machalski 2008, in preparation). The errors are calculated by

means of uncertainties of the parameters (a, b, c) in the analytical forms $y = a + bx + cx^2$ or $y = a + bx + c \exp(\pm x)$, which are used to smooth the data points in the plots of y versus x , where $x \equiv \alpha_{\text{inj}}$ and y is equivalent to either t , $\log(Q_{\text{jet}})$, or $\log(Q_{\text{jet}}t)$ (cf. Figure 4b). These uncertainties were determined during the fitting procedure of a set of pairs (x, y) with the above forms. Therefore, the errors given in Table 2 do not account for uncertainties of the model’s free parameters, such as a_0 , β , Γ_c , etc., as well as that of the observational parameter AR. A possible influence of uncertainties of the above parameters on the DYNAGE predictions has been discussed in Machalski et al. (2007a). Because of limited radio spectral data for J1420–0545, we suppose that the quoted errors for this radio galaxy may be larger by a factor of 2.

4.3. Discussion of the results

The DYNAGE model solution for J1420–0545 strongly suggests that this radio galaxy is at least twice as young as other GRGs at redshifts of about 0.1, and that it evolved in an exceptionally low-density environment. The fitted value of ρ_0 is a factor of 100 lower than the central densities of typical host galaxies themselves, (e.g. Canizares et al. 1987; Mulchaey & Zabludoff 1998; Hardcastle & Worrall 2000) and lower than the halo densities in clusters of galaxies, (e.g. Jones & Forman 1984; Schindler et al. 1999). In particular, the value of ρ_0 found for J1420–0545 is about 20 times lower than that for 3C236 (cf. Table 2). Enlarging the cocoon’s width, i.e. assuming that AR=8, causes a further decrease of the fitted value of ρ_0 by a factor of 3.4. On the other hand, the above enlargement does not change significantly the model solutions for the values of α_{inj} and t . For either value of AR, the minimum of the jets’ kinetic energy is at an α_{inj} value of around 0.48, and the age estimate is around 45 Myr. Such a relatively young age seems to be confirmed by evident hot spots that were clearly visible in both of the lobes of the source when it was mapped using the FIRST survey.

Having modeled the values of age and jet power with DYNAGE, we can estimate the value of the IGM (ambient) density at the jet heads, ρ_a . Balancing the ram pressure of the IGM and the thrust of the jet, Begelman & Cioffi (1989) derived the equation for the age of a FR type II source (their eq. [3]),

$$t \approx \left(\frac{\rho_a}{Q_{\text{jet}} v_{\text{jet}} A_h} \right)^{1/4} A_c,$$

where A_h and A_c are the cross-sectional areas of the bow shock at the head of the jet and of the cocoon, respectively. Thus, if we assume that the jet speed is close to the speed of

light and take into account that the areas A_h and A_c can be derived from the radio maps, a value of ρ_a can be calculated from the above equation. Usually A_h is identified with the cross-sectional area of hot spots. The deconvolved lateral angular sizes of the hot spots in the lobes of J1420–0545 are $3.8''$ and $4.1''$. Averaging these values, we find that their mean diameter is 17.7 kpc; hence, $A_h=2.34 \times 10^{41} \text{ m}^2$, whereas $A_c=1.14 \times 10^{44} \text{ m}^2$ for $AR=12$. Substituting these values of A_h and A_c , as well as the values of t and Q_{jet} from Table 2, into the above equation, we find that $\rho_a=5.9 \times 10^{-28} \text{ kg m}^{-3}$. If the cocoon were $(1.5)^2$ times fatter (i.e. if $AR=8$), the resulting ambient density would be lower by a factor of about 37 and would reach an unacceptably low value of about $1.6 \times 10^{-29} \text{ kg m}^{-3}$. Such a low value of AR is also very unlikely because the ambient density of $1.6 \times 10^{-29} \text{ kg m}^{-3}$ would correspond to that calculated from the density profile $\rho_a(r_h)=\rho_0(r_h/a_0)^{-\beta}$ at a radius of $r_h \approx 2.2 \text{ Mpc}$! A power-law density distribution at such a very large distance from the host galaxy is absolutely improbable. On the other hand, the value of $5.9 \times 10^{-28} \text{ kg m}^{-3}$ seems to be reasonable as it corresponds to a halo radius of $r_h \approx 445 \text{ kpc}$. This radius is well within the range of radii estimated for clusters of galaxies by Jones & Forman (1984).

There is also the possibility that the gaseous halo of the host galaxy is much smaller, and although the halo’s density profile in the case of J1420–0545 is not known, its jets may propagate through the (nearly) uniform IGM for a considerable fraction of the entire source lifetime. Therefore, while assuming that the source dynamics has been governed by the uniform environment, i.e. $\beta=0$, leads to an unphysical picture that the density at the head of jets, 2.2 Mpc away from the host galaxy, would be equal to its central density, it may be worthwhile to check how the fitted parameters of the source, i.e., the density in the front of the jets, ρ_a , the jets’ power, and the source age, would change if β was equal to zero (still for $AR=12$).

As a result, we find that Q_{jet} would be almost twice as strong as its value in Table 2, and the ambient density ρ_a would be lower by a factor of 4 than $5.9 \times 10^{-28} \text{ kg m}^{-3}$. Moreover, the source would be also younger than 47 Myr, which, in turn, would imply some even higher average expansion velocity of the source along the jet axis than the value provided in Table 2. The fitted values of the above parameters are given in Table 3. Certainly, an average expansion velocity of about $0.21 c$ (even $0.163 c$) is terribly higher than its values inferred from the spectral-ageing analyses for extended FR type II radio sources (e.g. Alexander & Leahy 1987; Liu et al. 1992) and for FR type II GRGs (Jamrozy et al. 2008), but it is rather similar to the advance speeds of sources not larger than 10–20 kpc (cf. Murgia et al. 1999). Although the dynamical age of lobes can be significantly higher than the synchrotron age of the oldest radiating particles (cf. Machalski et al. 2007a), such a high advance speed of J1420–0545 is quite an unexpected and puzzling result, because if the external density decreases more slowly than r^{-2} (where r is the distance from the core; cf. § 4.2), which is

the necessary condition for forming the head of the jet and to observe a source of FR type II, the advance speed does decrease with the source’s age (e.g. Falle 1991). Thus the above result may imply that the head of the jets in our galaxy must have propagated with a speed characteristic for very young compact double sources, or even comparable to the speed of light, not too long ago. This is evidently related to the very low density of the IGM found in the modelling.

There are two possible explanations that could account for lowering the true age of the source and enhancing its expansion speed:

1. Large errors in the flux densities used to calculate the radio luminosity of the lobes (cocoon) at the two observing frequencies. If the radio spectrum determined from these flux densities is flatter than the actual one, the source will appear younger in the modelling procedure;

2. Not all the kinetic energy in the jet flow had been transferred to the magnetic field and the relativistic electrons in the lobes. Such a situation is actually foreseen in the KDA model, in which the ratio (k') of the energy densities of thermal particles to that of electrons when they are spread into the cocoon during the injection is defined.

In order to provide a quantitative check of the possible influence of the uncertain radio spectrum, we generated a fiducial spectrum steeper than that derived from the observations available to date and ran the fitting procedure for the frequency range 150–4800 MHz. We found that the age of J1420–0545 could possibly rise to no more than 60 ± 7 Myr.

Following Kaiser et al. (1997), up to this point we have neglected any influence of the thermal particles in the lobes of J1420–0545; i.e. $k'=0$ was assumed. However, in order to check how the thermal plasma can modify the model parameters derived from the fit, we performed comparison calculations in which we set $k'=1$ and $k'=10$. The results are given in the last two rows of Table 3. It appears that all the parameters Q_{jet} , ρ_0 , ρ_a , u_c , p_c , and t do increase with k' , while, on the other hand, an increase of k' causes a decrease of the advance speed of the lobes. We note that the age t increases in a much slower manner than do the other parameters. Thus, a very high value of k' ($k=k' \gg 10$) would be necessary to reduce the advance speed of the galaxy to $0.01c$ – $0.04c$ (i.e. the values typical for the extended double radio sources; cf. Blundell et al. 1999), but speeds as high as $0.10c$ – $0.15c$ are not ruled out on the basis of the observed asymmetries of sources (Scheuer 1995). Also, the jets may not keep expanding with a constant opening angle and it is not at all clear that the velocities will keep systematically decreasing. The hot spot size seems to increase with the overall source size until about 10–20 kpc, after which it appears to be more constant (cf. Jeyakumar & Saikia 2000). In that paper the authors listed sources that had observational

evidence of reclamation of the jets. In such instances, the hot spot size would be smaller, which would increase the pressure due to the beam in the hot spots. It may also be important perhaps that J1420–0545 has significant hot spots, unlike most of the known giants, whose lobe structures are relatively diffused.

To summarize, we argue that the fitted parameters for J1420–0545 as given in Table 2 seem to be quite realistic ones, and the current uncertainty of its radio spectrum and the unknown influence of thermal plasma are not likely to significantly change the values derived in this paper. The very low ambient density around the lobes of our GRG strongly supports a hypothesis of large heterogeneity of the IGM.

4.4. Comparison to other radio galaxies of different linear size

In order to compare the derived parameters of J1420–0545 with the corresponding parameters of other FR type II radio galaxies we use the sample of 30 GRGs and 120 normal-sized galaxies (NSGs) analyzed by Machalski & Jamrozy (2006), for which dynamical age is determined with the DYNAGE. These data are supplemented with 17 small-sized double radio galaxies of the CSO and MSO types (compact and medium symmetric objects) for which the DYNAGE algorithm has given satisfactory results (J. Machalski 2008, in preparation). Figure 5 shows how the estimated parameters of J1420–0545 differ from the relevant parameters of other sources used for comparison. For example, the energy density of its lobes/cocoon, u_c , as well as the corresponding pressure, p_c , are extremely low (Figure 5a). The value of p_c (in Table 2) is a factor of 2.5 lower than that for 3C236, although the redshifts of J1420–0545 and 3C236 differ by a factor of 3. This confirms that J1420–0545 actually traces very low density environments. The ambient density at the head of the lobes, calculated from the dynamical arguments in §4.3 corresponds to a particle (proton) density of $\sim 10^{-7} \text{ m}_p \text{ cm}^{-3}$.

Furthermore, Figure 5b shows that GRGs are characterized by much lower radio luminosities than are NSGs of the same jet power. This is what one expects using the KDA model. The model predicts that the luminosity in the inverse-Compton-dominated regime decreases as $D^{-(4+\beta)(\frac{1}{3}+\Gamma_B)/3\Gamma_c}$ or $t^{-(4+\beta)(\frac{1}{3}+\Gamma_B)/\Gamma_c(5-\beta)}$, where Γ_B is the adiabatic index of a magnetic "fluid" and is equal to 4/3. Thus, for the assumed value of $\beta=1.5$ and $\Gamma_c=5/3$, one finds that $P_\nu \propto D^{-11/6}$ or $P_\nu \propto t^{-11/7}$. Figure 5b shows that J1420–0545 is less luminous than NSGs with a comparable jet power by a factor of about 100. Applying the predicted luminosity evolution with size D , one would expect J1420–0545 to have had the same luminosity as those NSGs when its linear size was about 380 kpc. On the other hand, a similar approach to the luminosity evolution with age t suggests that the investigated radio galaxy

would have had a luminosity that was higher by a factor of 100 when it was 2.5 Myr old. However, among 167 sources in the sample included in Figure 5, there are none that are both younger than 10 Myr and have a size larger than 200 kpc. It can be calculated that in this sample there is no source with $\rho_0 < 6 \times 10^{-25} \text{ kg m}^{-3}$ and only three with $\rho_0 \leq 10^{-24} \text{ kg m}^{-3}$. Therefore, although the largest radio galaxies can likely have evolved from younger and smaller sources, J1420–0545 is evidently a nontypical GRG due to its exceptionally low-density (a void?) environment as found by the fit.

The authors thank the Service Programme staff for the WHT observations, Alex Kraus for his help with the Effelsberg observations, and Michal Siwak for the Mount Suhora observations, as well as the Centre Director of the NCRA, TIFR, for the allocation of discretionary observing time and Chiranjib Konar for his assistance. The authors appreciate the comments and helpful suggestions of the anonymous referee. The Digitized Sky Surveys were produced at the Space Telescope Science Institute under US government grant NAG W-2166. The images of these surveys are based on photographic data obtained using the Oschin Schmidt Telescope on Palomar Mountain and the UK Schmidt Telescope. This work was supported in part by the Ministry of Science and Higher Education of Poland (MNiSW) with funds for scientific research in 2005-2007 under contract 5425/PO3/2005/29. D.K.-W. was partly supported by MNiSW funds for scientific research in 2007-2008 under contract 4272/H03/2007/32.

REFERENCES

- Alexander, P., & Leahy, J.P., 1987, MNRAS, 225, 1
- Becker, R.H., White, R.L., & Helfand, D.J., 1995, ApJ, 450, 559
- Begelman, M.C., & Cioffi, D.F., 1989, ApJ, 345, L21
- Blundell, K.M., Rawlings, S., & Willott, C.J., 1999, AJ, 117, 677
- Canizares, C.R., Fabbiano, G., & Trinchieri, G., 1987, ApJ, 312, 503
- Condon, J.J., Cotton, W.D., Greisen, E.W., Yin, Q. F., Perley, R. A., Taylor, G. B., & Broderick, J. J. 1998, AJ, 115, 1693
- Daly, R.A., 1990, ApJ, 355, 416
- Falle, S.A.E.G., 1991, MNRAS, 250, 581

- Hardcastle, M.J., & Worrall, D.M., 2000, MNRAS, 319, 562
- Jamrozy, M., Konar, C., Machalski, J. & Saikia, D.J., 2008, MNRAS, 385, 1286
- Jeyakumar, S. & Saikia, D.J., 2000, MNRAS, 311, 397
- Jones, C., & Forman, W., 1984, ApJ, 276, 38
- Kaiser, C.R., & Alexander, P., 1997, MNRAS, 286, 215
- Kaiser, C.R., Dennett-Thorpe, J., Alexander, P., 1997, MNRAS, 292, 723 [KDA]
- Lara, L., Márquez, I., Cotton, W.D., Feretti, L., Giovannini, G., Marcaide, J. M., & Venturi, T. 2001, A&A, 378, 826
- Leahy, J.P., & Williams, A. G., 1984, MNRAS, 210, 929
- Liu, R., Pooley, G. & Riley, J.M., 1992, MNRAS, 257, 545
- Machalski, J., & Jamrozy, M., 2006, A&A, 454, 95
- Machalski, J., Chyży, K.T., Stawarz, L., & Koziel, D., 2007a, A&A, 462, 43
- Machalski, J., Koziel-Wierzbowska, D., & Jamrozy, M., 2007b, A&A, 57, 227
- Mulchaey, J.S., & Zabludoff, A.I., 1998, ApJ, 496, 73
- Murgia, M., Fanti, C., Fanti, R., Gregorini, L., Klein, U., Mack, K.-H. & Vigotti, M., 1999, A&A, 345, 769
- Nath, B.B., 1995, MNRAS, 274, 208
- Scheuer, P.A.G., 1995, MNRAS, 277, 331
- Schindler, S., Binggeli, B., & Böhringer, H., 1999, A&A, 343, 420
- Schoenmakers, A.P., van der Laan, H., Röttgering, H.J.A., & de Bruyn, A. G. 1998, in ASP Conf. Ser. 146, The Young Universe, ed. S. O'dorico, A. Fontana, & E. Giallongo (San Francisco: ASP), 84
- Wellman, G.F., Daly, R.A., & Wan, L., 1997, ApJ, 480, 79

Table 1: Spectral Features Detected and Their Redshifts

Line/Absorption Band Detected	λ_{obs} (\AA)	z_{λ}
[O II] $\lambda 3727$	4870.9	0.3069
Ca II $\lambda 3934$	5142.1	0.3071
Ca II $\lambda 3968$	5185.6	0.3069
G band $\lambda 4305$	5622.0	0.3059
Mg band $\lambda 5175$	6762.0	0.3067

Table 2: Physical Parameters of J1420–0545 (for AR=12) and 3C236 (AR=16)

Parameter	Symbol/Relation	Value for J1420–0545	Value for 3C236
Initial effective spectral index	α_{inj}	0.477 ± 0.007	0.486 ± 0.009
Age	t [Myr]	47 ± 6	110 ± 18
Jet power	Q_{jet} [W]	$(2.91 \pm 0.30) \times 10^{38}$	$(1.88 \pm 0.20) \times 10^{38}$
Core density	ρ_0 [kg m^{-3}]	$(1.78 \pm 0.35) \times 10^{-25}$	$(3.73 \pm 0.45) \times 10^{-24}$
Kinetic energy	$2Q_{\text{jet}} t$ [J]	$(8.50 \pm 0.90) \times 10^{53}$	$(6.24 \pm 0.64) \times 10^{53}$
Energy density	u_c [J m^{-3}]	$(0.36 \pm 0.02) \times 10^{-14}$	$(0.89 \pm 0.05) \times 10^{-14}$
Internal pressure	p_c [N m^{-2}]	$(2.40 \pm 0.13) \times 10^{-15}$	$(5.94 \pm 0.33) \times 10^{-15}$
Magnetic field	B_c [nT]	0.062 ± 0.010	0.098 ± 0.014
Ratio of energy delivered/radiated	$2Q_{\text{jet}} t / u_c V_c$	14.2 ± 4.8	21.2 ± 5.1
Expansion speed	$D / (2 ct)$	0.163 ± 0.021	0.065 ± 0.010

Table 3: The Influence of the Values of β and k' on the Basic Physical Parameters.

β	k'	Q_{jet} (W)	ρ_0 (kg m^{-3})	ρ_a (kg m^{-3})	u_c (J m^{-3})	t (Myr)	$D/(2ct)$
0	0	5.37×10^{38}	1.55×10^{-28}	4.20×10^{-28}	0.20×10^{-14}	37 ± 3	0.207
1.5	0	2.91×10^{38}	1.78×10^{-25}	5.90×10^{-28}	0.36×10^{-14}	47 ± 6	0.163
	1	4.04×10^{38}	3.00×10^{-25}	1.05×10^{-27}	0.54×10^{-14}	50 ± 5	0.153
	10	8.63×10^{38}	1.28×10^{-24}	5.66×10^{-27}	1.46×10^{-14}	63 ± 8	0.121

Note. — In the solution for $\beta = k' = 0$, we have $\rho_0 < \rho_a$, where all the values of ρ_a are calculated from the eq. (3) of Begelman & Cioffi (1989).

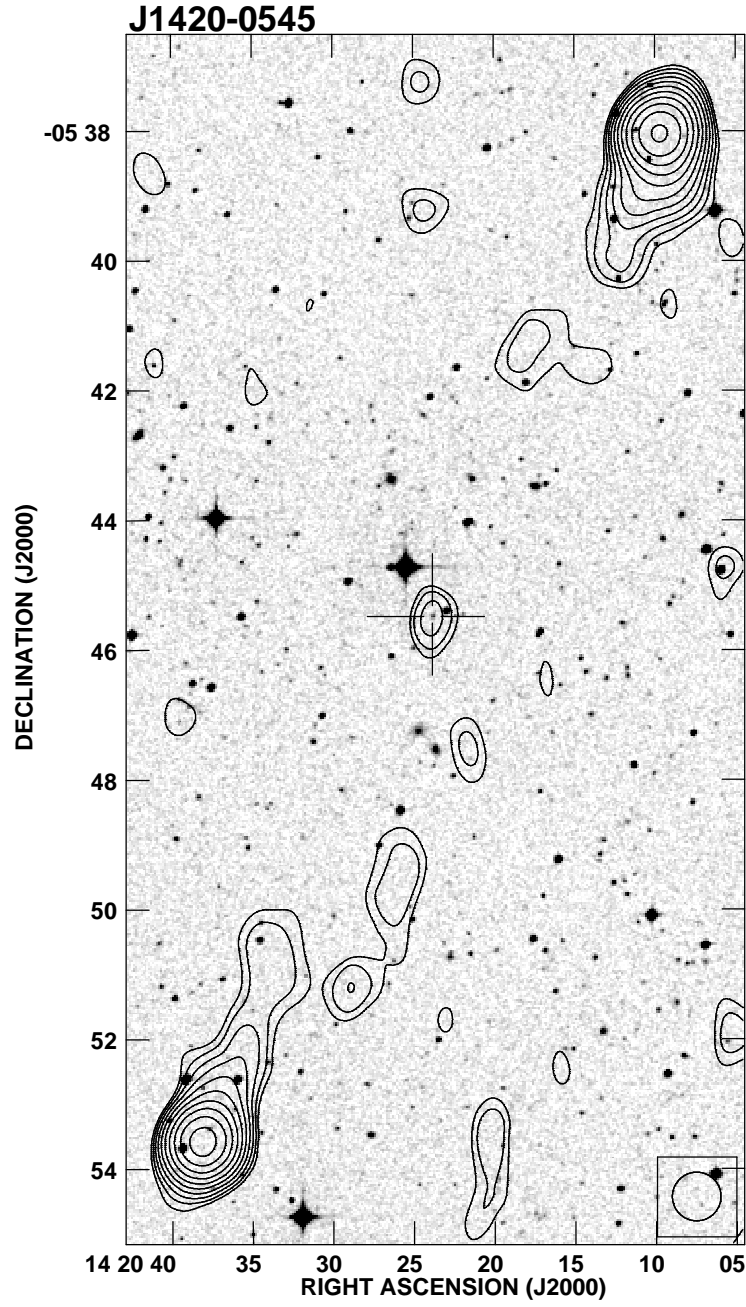


Fig. 1.— VLA and Effelsberg contour map of J1420–0545 at 1.4 GHz, superposed on the optical DSS field. Contours are logarithmic with a ratio of $2^{1/2}$ between levels; the first contour is at 1 mJy beam^{-1}

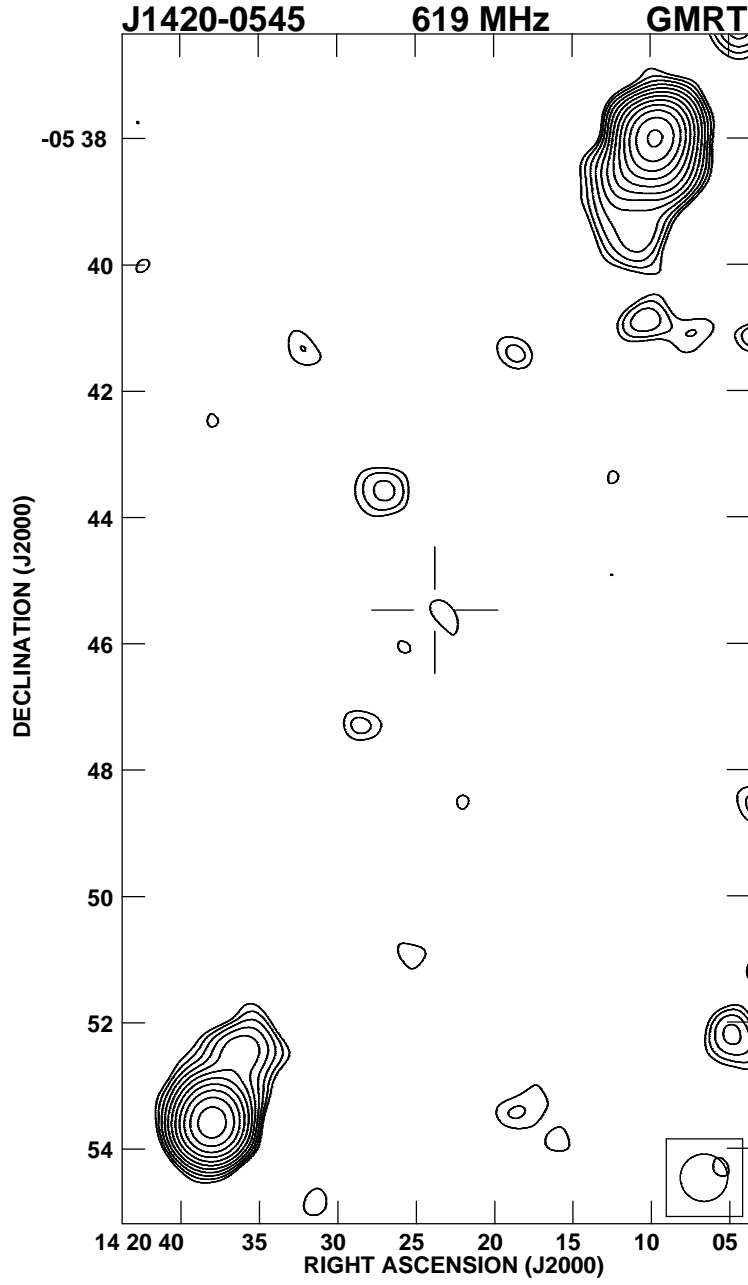


Fig. 2.— GMRT contour map of J1420–0545 at 619 MHz. Contours are logarithmic with a ratio of $2^{1/2}$ between levels; the first contour is at $1.3 \text{ mJy beam}^{-1}$

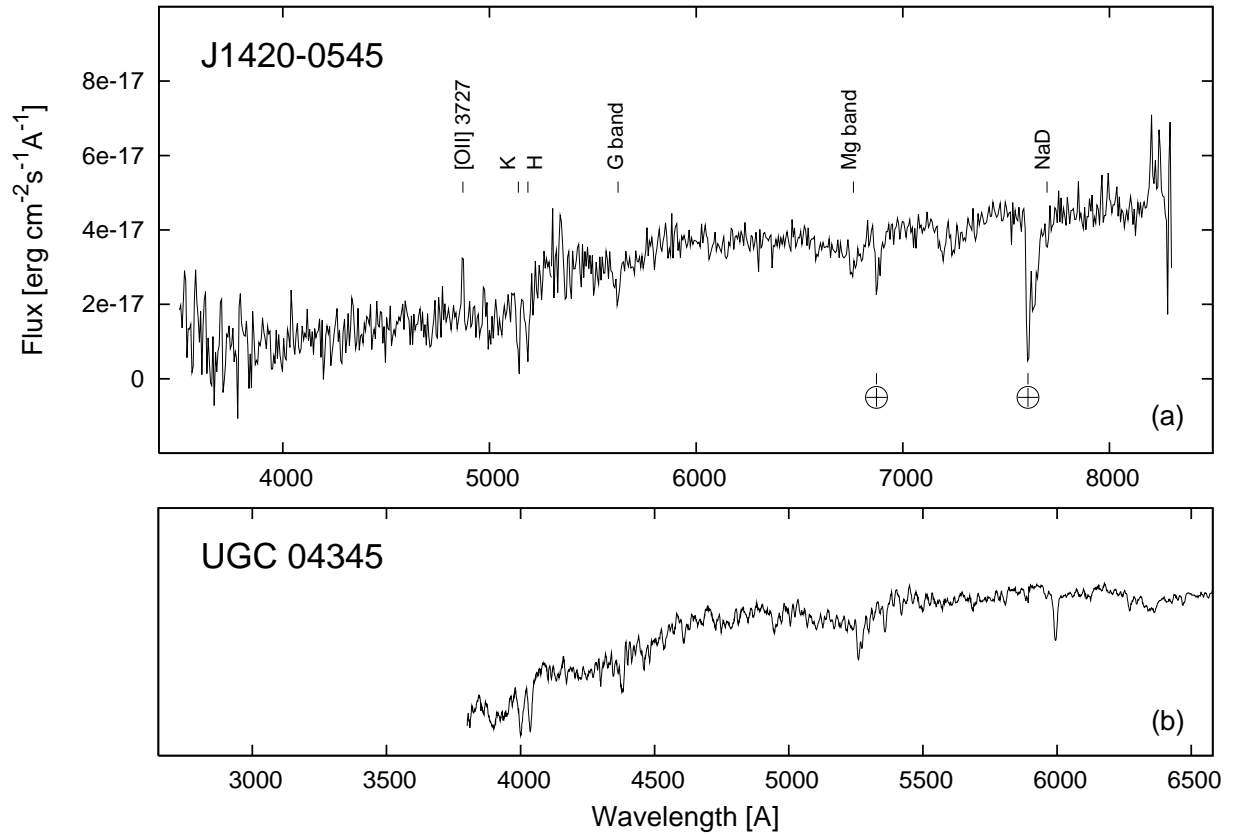


Fig. 3.— (a) Optical spectrum of J1420–0545. (b) Typical spectrum of an early-type radio-quiet galaxy, for comparison

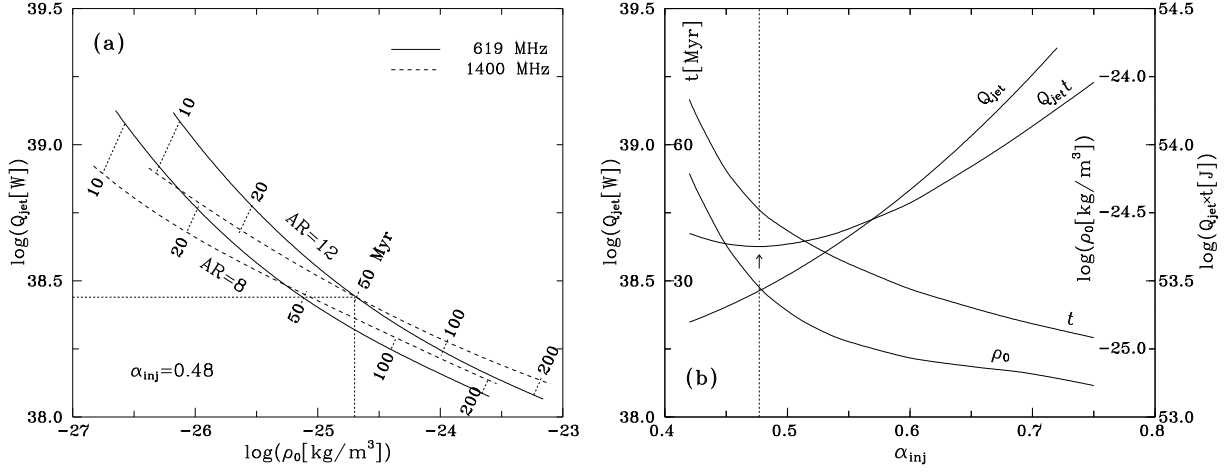


Fig. 4.— (a) Jet power vs. central core density ($Q_{\text{jet}} - \rho_0$) diagram at the two observing frequencies, for $\alpha_{\text{inj}}=0.48$ and two different values of AR. An intersection of the solid and dashed curves indicates an age solution and gives the corresponding values of Q_{jet} and ρ_0 for a given value of α_{inj} value. The dotted lines indicate the age to which the fitted values of Q_{jet} and ρ_0 are related. (b) Fitted values of age t as well as Q_{jet} , ρ_0 , and $Q_{\text{jet}} \times t$, as a function of α_{inj} . The arrow points to a minimum of the product $Q_{\text{jet}} t$ (i.e. a minimum of the total kinetic energy delivered to the cocoon by the jet), and the vertical dotted line indicates the corresponding value of α_{inj} that determines the best solution for the age.

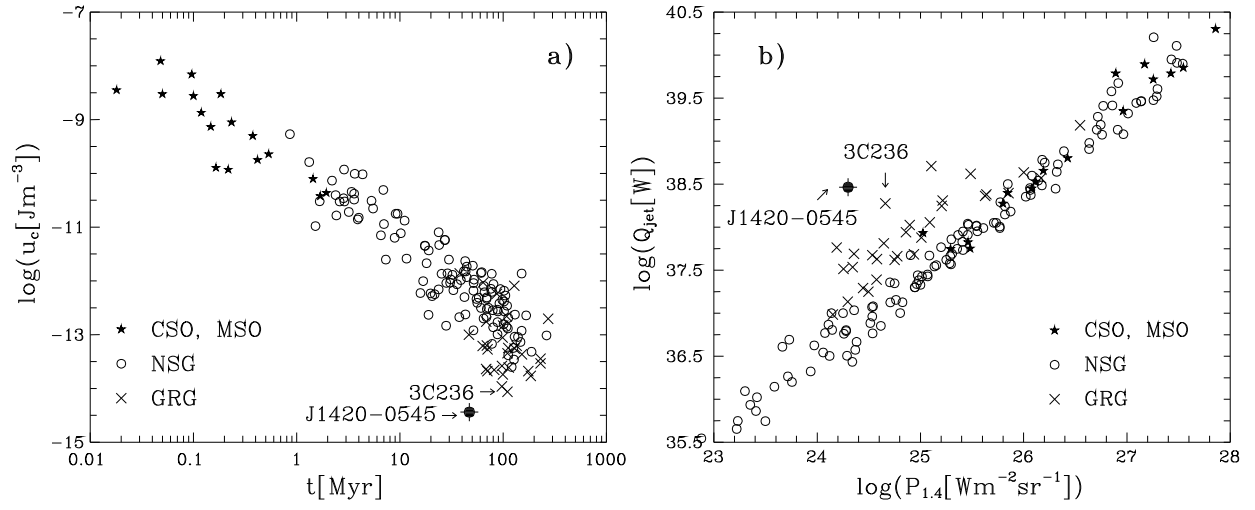


Fig. 5.— Loci of J1420–0545 on the diagrams of *a*) energy density of the source vs. its age and *b*) the jet power vs. the 1.4 GHz luminosity, comprising FR type II radio galaxies of different linear sizes